Histopathology and Functional Correlations in a Patient with a Mutation in *RPE65*, the Gene for Retinol Isomerase

Vera L. Bonilha,[1] Mary E. Rayborn,[1] Yong Li,[1,2] Gregory H. Grossman,[1] Eliot L. Berson,[3] and Joe G. Hollyfield[1]

PURPOSE. Here the authors describe the structural features of the retina and retinal pigment epithelium (RPE) in postmortem donor eyes of a 56-year-old patient with a homozygous missense *RPE65* mutation (Ala132Thr) and correlate the pathology with the patient's visual function last measured at age 51.

METHODS. Eyes were enucleated within 13.5 hours after death. Representative areas from the macula and periphery were processed for light and electron microscopy. Immunofluorescence was used to localize the distribution of RPE65, rhodopsin, and cone arrestin. The autofluorescence in the RPE was compared with that of two normal eyes from age-similar donors.

RESULTS. Histologic examination revealed the loss of rods and cones across most areas of the retina, attenuated retinal vessels, and RPE thinning in both eyes. A small number of highly disorganized cones were present in the macula that showed simultaneous labeling with cone arrestin and red/green or blue opsin. RPE65 immunoreactivity and RPE autofluorescence were reduced compared with control eyes in all areas studied. Rhodopsin labeling was observed in rods in the far periphery. The optic nerve showed a reduced number of axons.

CONCLUSIONS. The clinical findings of reduced visual acuity, constricted fields, and reduced electroretinograms (ERGs) 5 years before death correlated with the small number of cones present in the macula and the extensive loss of photoreceptors in the periphery. The absence of autofluorescence in the RPE suggests that photoreceptor cells were probably missing across the retina for extended periods of time. Possible mechanisms that could lead to photoreceptor cell death are discussed. (*Invest Ophthalmol Vis Sci.* 2011;52:8381–8392) DOI:10.1167/iovs.11-7973

From the [1]Cole Eye Institute, Department of Ophthalmology, Cleveland Clinic Lerner College of Medicine, Cleveland, Ohio; and the [3]Berman-Gund Laboratory for the Study of Retinal Degenerations, Harvard Medical School, Massachusetts Eye and Ear Infirmary, Boston, Massachusetts.

[2]Present affiliation: Department of Neurological Surgery, Case Western Reserve University, Cleveland, Ohio.

Leber congenital amaurosis (LCA) comprises a group of genetic disorders in which visual loss or dysfunction is present at birth. Patients typically have hyperopia and nystagmus and reduced electroretinograms (ERGs). The extent of visual loss varies from patient to patient but is usually severe. Mutations have been identified in 15 genes in persons with LCA, each of which is a recessive disorder.[1,2]

Mutations in the *RPE65* gene account for approximately 7% of LCA. *RPE65* is uniquely expressed in the retinal pigment epithelium (RPE), where the protein, an enzyme, binds and converts all-*trans* retinyl ester to 11-*cis* retinol.[3–5] Retinol isomerization is an essential enzymatic step required for functional vision to occur in rod and cone photoreceptors.[6,7] More than 60 mutations in the *RPE65* gene have been documented in LCA patients. Mutations have been reported in each of the 14 exons of the *RPE65* gene and its boundaries.[8–14] Typically, mutations in the *RPE65* gene result in impaired vision from birth and typically progress to legal blindness in the third decade of life.[9,11,12,15,16]

Mutations in *RPE65* do not necessarily result in early loss of photoreceptors. For example, studies of dog retinas with a naturally occurring *RPE65* mutation and mouse retinas that are missing the *RPE65* gene show structurally intact photoreceptors visible by optical coherence tomography that appear nonfunctional because of the inability of the RPE to generate 11-*cis* retinal. The sparing of photoreceptors has allowed *RPE65* gene replacement therapy to restore this critical retinol isomerase activity to the RPE with the accompanying restoration of visual function.[17,18]

In this report we describe the pathology and clinical findings in a woman with a homozygous mutation (Ala132Thr) in the *RPE65* gene.[12] Unlike most persons with RPE65 mutations, this patient retained some vision into her early fifties. To our knowledge this is the first study of adult postmortem donor eyes from a patient with a homozygous recessive mutation in the *RPE65* gene.

METHODS

Clinical evaluations were carried out at the Harvard Medical School, Massachusetts Eye and Ear Infirmary (Boston, MA). The research conformed to the tenets of the Declaration of Helsinki.

Tissue Acquisition and Fixation

The patient was a registered eye donor with the Foundation Fighting Blindness and the Berman-Gund Laboratory. Eyes were enucleated 13.5 hours postmortem and fixed in 4% paraformaldehyde and 0.5% glutaraldehyde in phosphate buffer. After 1 month in fixative, the globes were transferred and stored in 2% paraformaldehyde in PBS. Normal postmortem donor eyes from a 60-year-old woman and a 61-year-old man were used as controls.

Immunohistochemistry

Small areas from the macula (OD and OS) and peripheral eye wall (OD) were cut and infused successively with 10% and 20% sucrose in PBS, and embedded in optimum temperature cutting compound (Tissue-Tek 4583; Miles Inc., Elkhart, IN). Ten-micrometer cryosec-

tions were cut on a cryostat (HM 505E; Microm, Walldorf, Germany) equipped with a tape-transfer system (CryoJane; Instrumedics, Inc., Hackensack, NJ). Before labeling, embedding medium was removed through two consecutive PBS incubations for 20 minutes. The tissue was then processed for immunofluorescence labeling. Sections
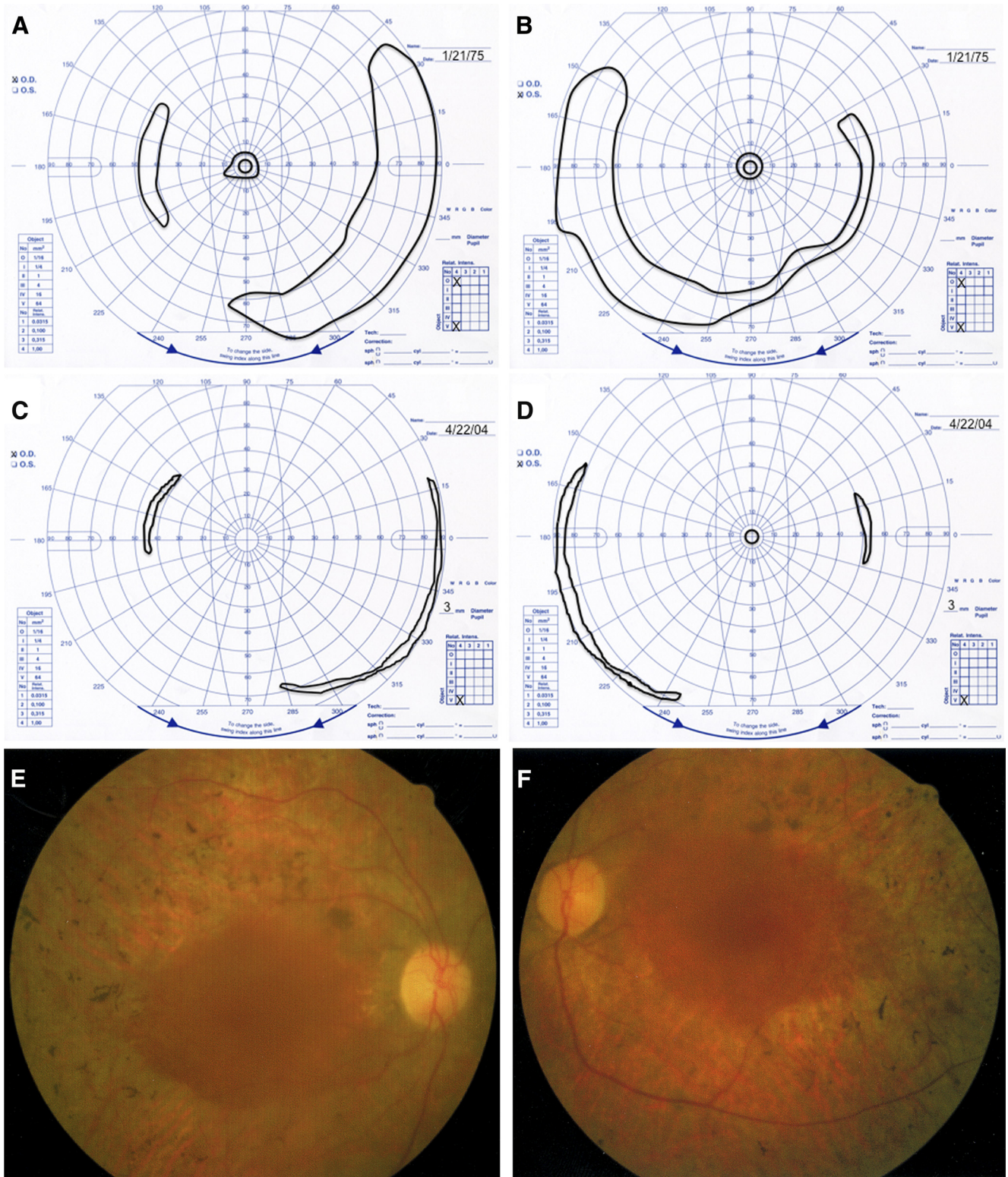
FIGURE 1. Findings in patient with RPE65 gene mutation. (**A**, **B**) Goldmann visual fields to a V-4e white test light and I-4e white test light at age 22. (**C**, **D**) Goldmann visual fields to a V-4e white test light at age 51. (**E**, **F**) Fundus photographs OD and OS at age 51.

were blocked in PBS supplemented with 1% BSA (PBS/BSA) for 30 minutes and incubated with monoclonal antibody B6–30N to rhodopsin (1:100; from Paul Hargrave, University of Florida, Gainesville, FL) and polyclonal antibodies PETLET to RPE65 (1:500; from Rosalie Crouch, University of South Carolina, Charleston, SC), to red/green (AB5405, 1:1200; Chemicon), and to blue (AB5407, 1:1200; Chemicon, Temecula, CA) opsin, and monoclonal antibody 7G6 to cone arrestin (1:100; from Peter MacLeish, Morehouse School of Medicine, Atlanta, GA) in PBS/BSA overnight at 4°C. Cell nuclei were labeled with iodide (TO-PRO-3; blue, 1 mg/mL; Molecular Probes, Eugene, OR). Secondary antibody goat anti-mouse IgG (1:1000) was labeled with Alexa Fluor 488 (green; Molecular Probes) while goat anti-rabbit IgG was labeled with Alexa Fluor 488 or 594 (red) for 1 hour at room temperature. Sections were analyzed using a laser scanning confocal microscope (TCS-SP2; Leica, Exton, PA). A series of 1-μm *x-y* (en face) sections were collected. Each individual x-y image of the retinas stained represented a three-dimensional projection of the entire cryosection (sum of all images in the stack). Microscopic panels were composed using image editing software (Photoshop CS3; Adobe, San Jose, CA).

Immunofluorescence Montages

Sections labeled with antibodies to cones and rods were stained as described and were imaged with a fluorescence microscope (BX-61; Olympus, Tokyo, Japan) equipped with a charge-coupled device monochrome camera (Hamamatsu Photonics, Bridgewater, NJ). Each montage image represented a composition of a series of individual photomicrographs collected throughout the whole tissue with 10$\times$ and 20$\times$ objectives using a computer-controlled motorized x-y stage (Proscan II; Prior Scientific Inc., Rockland, MA) and reconstructed into one image (SlideBook software, version 4.2; Intelligent Imaging Innovations, Denver, CO).

Semithin Epon Sections and Ultrastructural Analysis

A small area of the retina/RPE/choroid tissue from both the macular region (OS) and the periphery (OD) of the RPE65 donor and matched-controls were fixed in 2.5% glutaraldehyde in 0.1 M cacodylate buffer, sequentially dehydrated in ethanol, and embedded in Epon. One-

micrometer plastic sections of both samples were stained with toluidine blue and examined and photographed by light microscopy with a microscope (Axiophot; Carl Zeiss, Jena, Germany) equipped with a high-sensitivity charge-coupled device camera (C5810; Hamamatsu Photonics, Hamamatsu, Japan). Thin sections were prepared, and electron micrographs were taken on a 200-kV digital electron microscope (Tecnai 20; Philips, Hillsboro, OR) using a Gatan (Pleasanton, CA) image filter and a digital camera at 3600 diameters and were printed at identical magnifications.
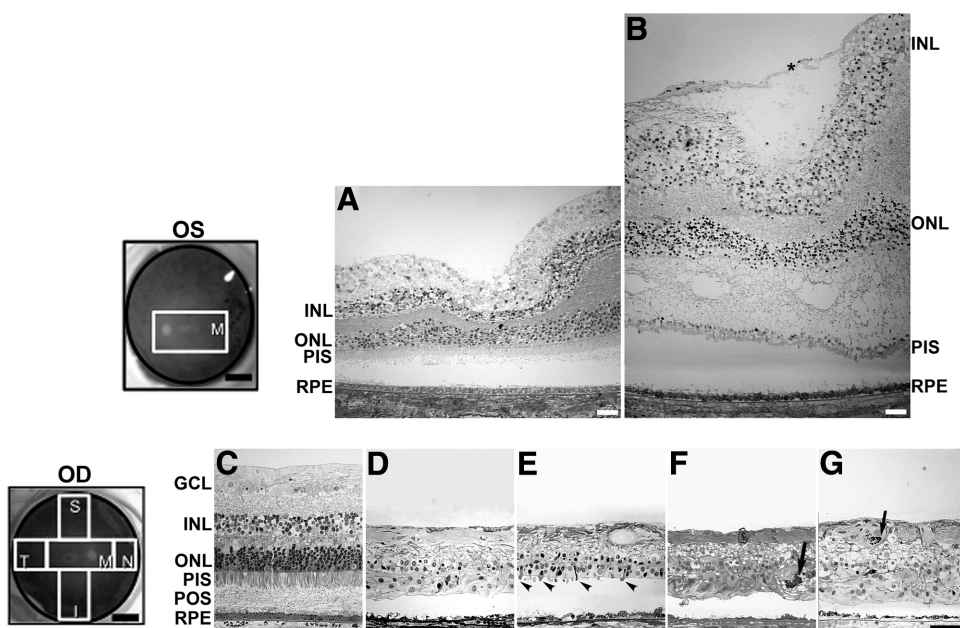
RESULTS

Clinical Findings

The patient was first examined by one of the authors (ELB) at age 22, at which time she reported night blindness and limited side vision since childhood. At the initial examination, she had best-corrected visual acuity of 20/40 (right eye, OD) and 20/30 (left eye, OS). Her visual fields were constricted to 11° diameter centrally, with peripheral islands in both eyes with a V-4e white test light (Figs. 1A, 1B). Slit lamp examination showed clear lenses in both eyes (OU). Fundus examination showed a normal disc, retinal arteriolar attenuation, and bone spicule pigmentation around the midperiphery in each eye. Dark adaptation OS with an 11° diameter white test light showed a threshold 3.5 log units above normal after 45 minutes of dark adaptation. Rod and cone responses were nondetectable (<10 μV) with conventional full-field ERG testing. With narrow bandpass filtering and computer averaging, full-field 30-Hz cone responses were 8.4 μV OU (lower normal is 50 μV).

She was most recently examined by us at age 51, 5 years before her death. At that time, she had hand motions vision OD and 20/200 OS. Visual field testing showed reduction of the temporal island in each eye, no detectable central field OD, and only a 4° central field diameter OS (Figs. 1C, 1D). Slip lamp examination revealed central posterior subcapsular cataracts in both eyes. Fundus examination of each eye showed slight waxy pallor of the disc, a granular macula, attenuated retinal vessels, and bone spicule pigmentation

FIGURE 2. Degeneration in the retina of an RPE65 donor. Fundus images of both eyes with disc and macula delineated; schematic drawing of the regions cut and processed for cryosectioning (*far left, top and bottom*). One-micrometer plastic sections of both matched control (**A, C**) and RPE65 donor (**B, D–G**) postmortem retinas stained with toluidine blue. The macula of the left eye of the RPE65 donor (**B**) displayed edema. It contained a prominent preretina (epiretinal) membrane composed of fibroblastlike cells that were vitread to a connective tissue lamina (*). In the periphery, the retina of the RPE65 donor (**D–G**) displayed different degrees of retinal degeneration in all quadrants observed. Sparse inner and outer nuclear layers with stunted photoreceptor inner and outer segments are evident in the superior quadrant (**E**, *arrowheads*). A few pigmented cells are seen invading the degenerating retina of the temporal (**F**) and nasal quadrant (**G**, *arrows*). Finally, a thin, continuous area of pigmented RPE cells was present. Quadrants: M, macula; I, inferior; S, superior; T, temporal; N, nasal. RPE, retinal pigment epithelium; POS, photoreceptor outer segment; PIS, photoreceptor inner segment; ONL, outer nuclear layer; INL, inner nuclear layer; GCL, ganglion cell layer. Scale bars: 0.5 cm (fundus images *upper* and *lower left*); 400 μm (**A, B**); 200 μm (**C–G**).

around the periphery (Figs. 1E, 1F). A small central macular hole could be visualized OD. No macular edema could be seen. Dark-adaptation OS showed a final threshold still elevated 3.5 log units above normal. Narrow band-passed, computer-averaged, 30-Hz cone ERGs were now only 0.50 μV (OD) and 0.67 μV (OS). Applanation tensions of 10 mm Hg (OD) and 12 mm Hg (OS) were recorded during her visit at age 51.

Histopathology of the Retina and Optic Nerve

Semithin sections of Epon-embedded RPE65 eye tissue were analyzed and compared with equivalent areas in an age-similar control eye (Fig. 2). A schematic drawing of the postmortem donor eye under study depicts the regions harvested and processed for both histologic and immunohistologic analysis: inferior (I), superior (S), temporal (T), nasal (N), retina, and macula (M). The macula of the left eye (Fig. 2B) was swollen. It contained a prominent preretinal (epiretinal) membrane composed of fibroblastlike cells that were vitreal to a connective tissue lamina. In each quadrant of the periphery, the retina (Figs. 2D–G) displayed different degrees of degeneration when compared with the morphology of the control retina in the periphery (Fig. 2C) and macula (Fig. 2A). No layers of nuclei (ganglion, inner, and outer) were evident in any of the quadrants of the retinal periphery analyzed. Nuclei were randomly distributed throughout the disorganized retina. The inner and outer plexiform layers were also not evident. An occasional stunted photoreceptor inner and outer segment projecting from the outer retinal surface was evident in the superior quadrant (Fig. 2E, arrowheads). A few pigmented cells were observed invading the degenerate retina of the temporal and nasal quadrants (Figs. 2F, 2G, arrows). The vitreal surface of the retina was formed of glial fibers ending at the inner limiting membrane. The RPE layer was continuous below the degenerate retina, but RPE cells had reduced apical to basal height compared with the RPE in age-similar control eyes.

Cross-sections of the optic nerve were taken approximately 1 mm behind the lamina cribrosa (Fig. 3). A few myelinated axons were found in the optic nerve of the RPE65 donor (Figs. 3B, 3D) compared with sections from the control nerves at equivalent retrolaminar locations (Figs. 3A, 3C). Only a few nuclei (possible astrocytes) were evident (Fig. 3D), and the diameters of the central retinal artery and vein were severely reduced in diameter (Fig. 3F) compared with control (Fig. 3E). The paucity of axons in the optic nerve was consistent with the absence of distinct ganglion cells in the RPE65 donor retina.
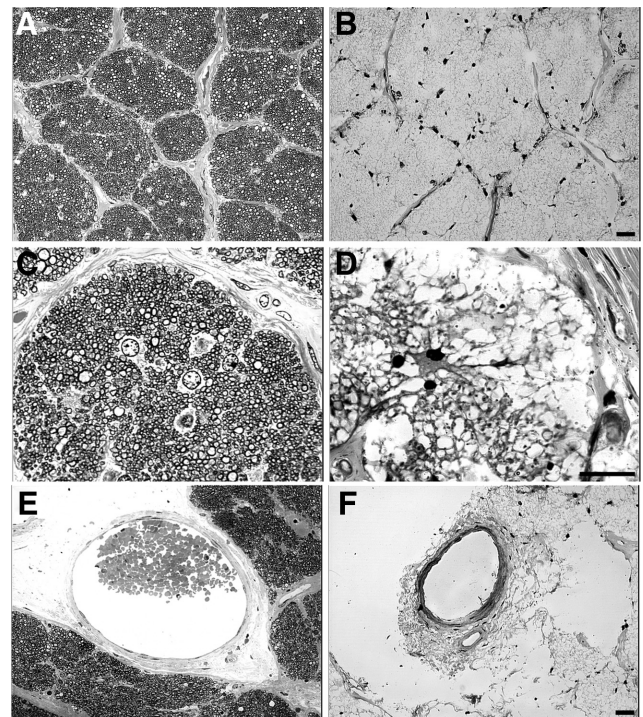
Immunohistocytochemistry Studies

The RPE65 postmortem donor eye displayed a continuous but much decreased signal of RPE65 immunoreactivity in the macula compared with the control eye (Figs. 4A–D). In some areas of the macula, multilayered RPE65-positive cells could be observed bulging into the subretinal space (Figs. 4E, 4F). In the peripheral retina, RPE65 immunoreactivity was patchy and sparse, probably related to the RPE attenuation and thinning (Figs. 4G, 4H).

To follow some of the specific molecular changes in the remaining photoreceptors, the retina of the postmortem RPE65 donor was also evaluated for the distribution of cone arrestin in the macula of each eye (Fig. 5) and in the periphery (Fig. 6). Cone arrestin distribution was compared with that in a control eye in similar regions. Individual images collected throughout the whole tissue length were acquired and reconstructed into a montage. In the RPE65 donor retina, a small cluster of foveal cones was still present in both eyes; these were highly disorganized and lacked distinct cone synaptic terminals (Fig. 5). In addition, cone arrestin–positive cells were

rarely observed in any peripheral retinal quadrant studied (Fig. 6). Therefore, our immunohistologic observations cannot account for the difference in vision acuity recorded when the patient was tested 5 years earlier.

In control retinas, cone arrestin antibody labeled the entire cone cell body in all retinal areas studied (Fig. 7). Observation at higher magnification showed that cone arrestin antibody labeled the few remaining cones in the fovea of the RPE65 eye, but cone pedicles were not labeled and could not be identified (Fig. 7B). Cone arrestin immunoreactivity was rarely encountered in the peripheral retina, which was consistent with the absence of all photoreceptor types in these locations. The few remaining cones exhibited amorphous morphology and expansion of the retina horizontally (Figs. 7C–F). Moreover, there was a paucity of nuclei in the outer nuclear layer labeled with iodide (TO-PRO-3; Molecular Probes) in the RPE65 eye compared with the control eye.

Cones were further characterized through double labeling of the macula (Fig. 8) and periphery (Supplementary Fig. S1; http://www.iovs.org/lookup/suppl/doi:10.1167/iovs.11-7973/-/DCSupplemental) with red/green or blue opsin and cone arrestin antibodies. As described, cone arrestin is distributed through the entire cytoplasm of cones (Figs. 8A, 8G; Supplementary Figs. S1A, S1G; http://www.iovs.org/lookup/suppl/doi:10.1167/iovs.11-7973/-/DCSupplemental) whereas red/green opsin (Fig. 8B; Supplementary Fig. S1B; http://www.iovs.org/lookup/suppl/doi:10.1167/iovs.11-7973/-/DC Supplemental) and blue opsin (Fig. 8H; Supplementary Fig. S1H; http://www.iovs.org/lookup/suppl/doi:10.1167/iovs.11-7973/-/DCSupplemental) are restricted to the outer segment in

FIGURE 3. Degeneration in the optic nerve of the RPE65 donor. Light microscopy of 1-μm plastic sections of optic nerve from both a matched control (**A**, **C**, **E**) and the RPE65 donor (**B**, **D**, **F**) stained with toluidine blue. Analysis of the optic nerve of the RPE65 donor in both low (**B**) and high (**D**) magnification showed the absence of myelinated axons when compared with the control (**A**, **C**). Only a few nuclei (astrocytes?) are evident (**D**). There is a paucity of axons consistent with the loss of ganglion cells in the retina. Finally, the RPE65 donor displayed a severely reduced central retinal vessel diameter (**F**). Scale bars, 200 μm.
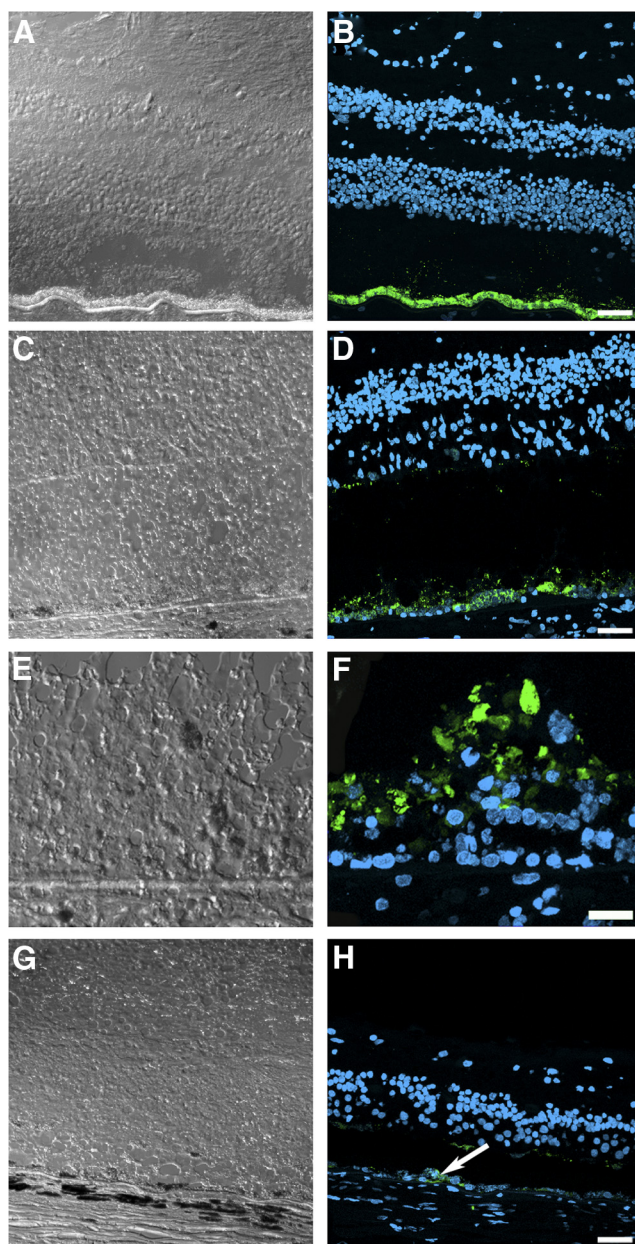
FIGURE 4. Presence of remaining RPE cells expressing RPE65 in the postmortem eyes from an RPE65 donor. A continuous layer of cells was observed expressing RPE65 in the control (**B**) and in the macula of the RPE65 donor (**D**); however, the RPE65 donor expression was substantially lower than that observed in the control tissue. In a few areas in the macula of the RPE65 donor (**F**), several layers of RPE65-positive cells were observed in the RPE65 donor retina. In the periphery of the RPE65 donor retina, very few cells were detected expressing RPE65 (**H**, *arrow*). **A**, **C**, **E**, and **G** are differential interference contrast microscopy images of the same field shown in **B**, **D**, **F**, and **H**. Scale bars, 40 μm (**B**, **D**, **H**); 20 μm (**F**).

control eyes. In the RPE65 eye, red/green opsin displayed a diffuse, cytoplasmic distribution in the macula (Fig. 8E) and retinal periphery (Supplementary Fig. S1E; http://www.iovs.org/lookup/suppl/doi:10.1167/iovs.11-7973/-/DCSupplemental). Interestingly, blue opsin displayed a decreased but membrane-associated distribution in the macula (Fig. 8K) and periphery (Supplementary Fig. S1K; http://www.iovs.org/lookup/suppl/doi:10.1167/iovs.11-7973/-/DCSupplemental) compared with the control tissue distribution. As described, cone arrestin

labeling in the RPE65 donor eye macula highlighted the abnormal distribution of cones (Figs. 8D, 8J) whereas in the periphery only severely degenerate cones remained (Supplementary Figs. S1D, S1J; http://www.iovs.org/lookup/suppl/doi:10.1167/iovs.11-7973/-/DCSupplemental).

Rod photoreceptors were identified with a rhodopsin antibody. After antibody labeling, individual overlapping images were collected throughout the entire tissue expanse from each retinal quadrant studied and were used to construct a montage (Fig. 9). Comparison of the samples showed that rhodopsin labeling was mostly absent in the RPE65 eye. A few rods were detected in the far periphery of the temporal quadrant of the RPE65 eye (Fig. 9D, arrows).

Rhodopsin is normally localized only to the outer segment (Fig. 10A), but in the few rods found in the RPE65 eye, rhodopsin was distributed throughout the entire cell body (Figs. 10B–F). Comparison of the samples showed that rods were significantly decreased in all the observed regions; the remaining rods had lost the normal rodlike shape and were much shorter than rods in control retinas. Additionally, rhodopsin-labeled neuritelike processes were commonly observed extending into the inner retina.

Photoactivation of rhodopsin and cone opsin results in the isomerization of 11-*cis* retinal to all-*trans* retinal, which is then recycled to the RPE for regeneration in a pathway termed the retinoid visual cycle. During aging, a functional visual cycle is necessary for the RPE to accumulate lipofuscin, the fluorescent storage material that accumulates in RPE cells. We compared the relative amount of autofluorescence in the RPE postmortem donor eye with control RPE. RPE in the macula (Fig. 11B) showed a substantial decrease of autofluorescence compared with RPE in the macula of the age-similar control eyes (Fig. 11A). Finally, in the periphery, the RPE in the RPE65 donor retina showed a paucity of autofluorescence (Figs. 11D–G) compared with an age-similar control RPE (Fig. 11C).
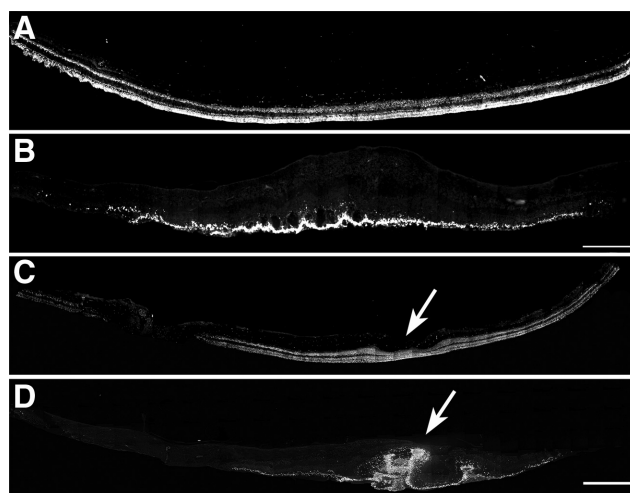
FIGURE 5. Presence of disorganized cones in the macular region of both postmortem eyes from an RPE65 donor. Montages of photomicrographs of the macular region of both the right (**B**) and the left (**D**) postmortem eyes from the RPE65 donor and control eyes (**A**, **C**) were analyzed using a cone arrestin antibody (7G6). Observations showed that in the RPE65 postmortem donor eyes, cones were still present in the macula but were highly disorganized and synapses were absent. (*arrows*) Macula pit. Scale bar, 500 μm.
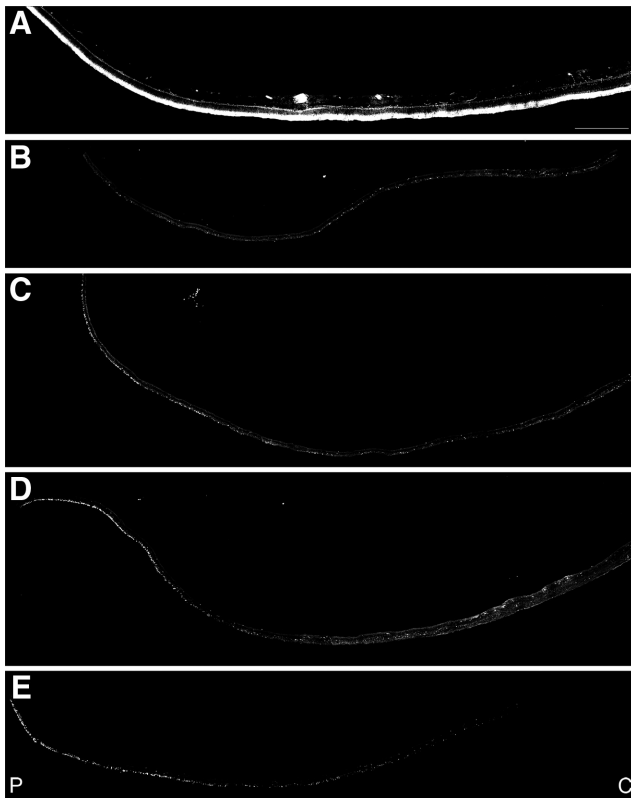
FIGURE 6. Significant reduction in the cones in the periphery of an RPE65 postmortem donor eye. Montages of photomicrographs of the periphery tissue from the RPE65 donor (**B–E**) and control eyes (**A**) were analyzed using a cone arrestin antibody (7G6). Comparison of the samples showed that cones were mostly absent in the affected retina in inferior (**B**), superior (**C**), temporal (**D**), and nasal (**E**) regions. P, periphery; C, central. Scale bar, 500 μm.

## Ultrastructural Studies of the RPE and Bruch's Membrane

Transmission electron microscopy of RPE and Bruch's membrane in the fovea (Figs. 12C, 12D) and periphery (Figs. 12E–H) of the RPE65 donor and an age-similar control eye (Figs. 12A, 12B) was performed, and findings were compared. The control RPE displayed the expected apical microvilli (Fig. 12A) and basal infoldings (Fig. 12B). In contrast, the RPE65 postmortem donor eye showed degenerative changes in the RPE in each quadrant studied. In the macula, apical microvilli were absent, and pleomorphic inclusions were common (Figs. 12C, 12D). In the nasal quadrant, apical microvilli were present (Fig. 12E); however, the basal region was characterized by the presence of electron-dense material beneath the RPE cells (Fig. 12F). In the inferior quadrant, inflammatory cells were present above the RPE in some areas (data not shown). A few short microvilli remained on their apical surface (Fig. 12G). Examination of the RPE basal surface revealed a complete absence of basal infoldings and the presence of a debris zone beneath the RPE. Bruch's membrane had lost the pentalaminate structure and was disorganized in this area (Fig. 12H).

DISCUSSION

This study reveals for the first time the histologic changes present in an adult retina of a patient with an RPE65 mutation. The Ala132Thr site mutation in exon 5 of the *RPE65* gene was previously identified in this patient and several family mem-

bers.[12] The functional consequence of this specific RPE65 mutation was also studied previously in vitro, in 293 cells.[5] Data showed that mutation to threonine at residue 132 lead to 50% reduction in the activity of isomerization potential of RPE65. Some remaining activity of RPE65 enzyme most likely contributed to the long retention of vision measured in this patient.

Several studies[19-21] have evaluated the retinas in RPE65-deficient (LCA) patients in vivo through the use of optical coherence tomography combined with visual function. These studies determined that despite severely reduced early loss of cone vision, many persons with *RPE65* mutations had near-normal foveal microstructure but most were lacking rods.[19-21] Observation of the fovea also showed that patients with RPE65 deficiency exhibited some cone photoreceptor loss, even at the youngest ages. However, residual cone photoreceptor function persisted for decades.[20] In fact, these patients have differing amounts of cone function, with some older patients having more function than younger patients.[20,22,23] Based on these studies it is likely that gene therapy will have to be targeted to different regions, possibly on a case-by-case basis.
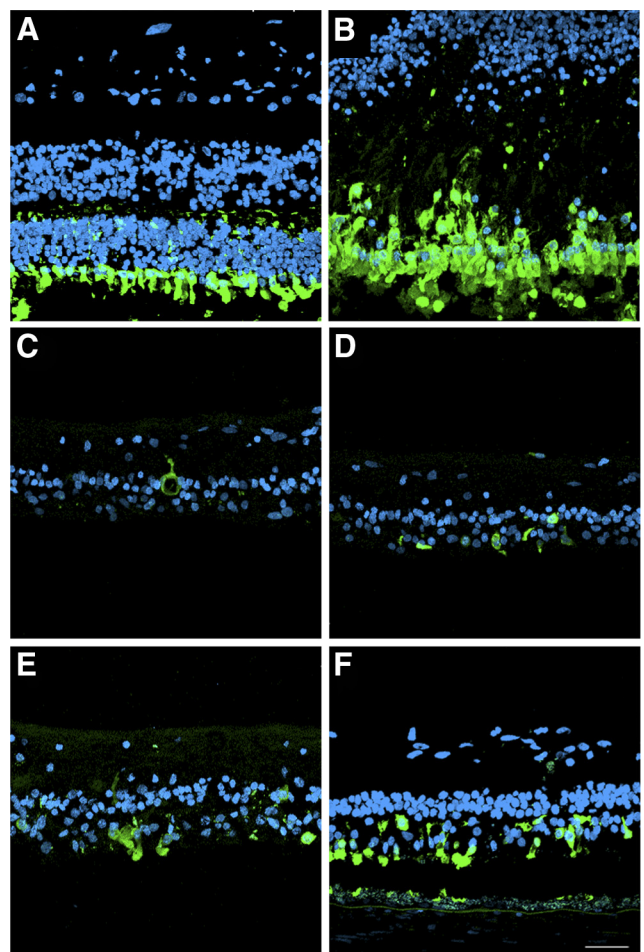
FIGURE 7. Disorganized morphology of the cones remaining in the retina of an RPE65 postmortem donor eye. High-magnification comparison of the control and RPE65 donor retina showed that cone arrestin was distributed along the entire plasma membrane of this cone type, from the tip of the outer segment to the synaptic base in the control retina (**A**). Cones were present in the macula of the RPE65 donor, but synapses were not visualized (**B**). On the other hand, cones were mostly absent in the periphery of the RPE65 mutant retina in the inferior (**C**), superior (**D**), temporal (**E**), and nasal (**F**) quadrants. Scale bar, 40 μm.
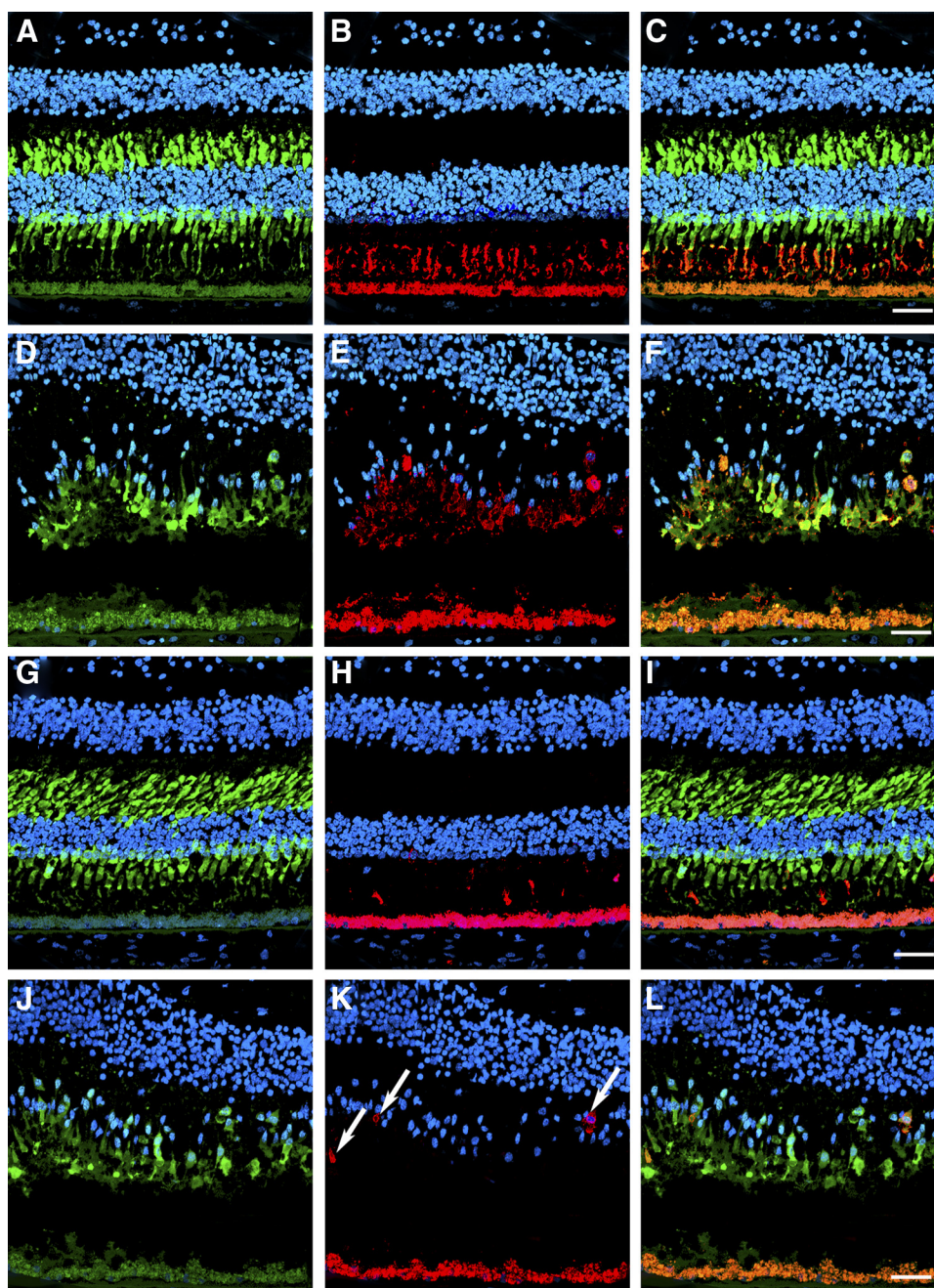
FIGURE 8.   Disorganized expression of red/green and blue opsins in the cones in the macula of an RPE65 postmortem donor eye. The distribution of cones was also analyzed in control and RPE65 eyes labeled with the cone arrestin (7G6), red/green opsin (AB5405), and blue opsin (AB5407) antibodies. Control retinas displayed cone arrestin distributed along the entire cone cell body (**A**, **G**), however the RPE65 donor retina displayed disorganized cones (**D**, **J**). In the control eyes, red/green (**B**) and blue (**H**) opsins were restricted to the cone outer segments. In the RPE65 eyes, the red/green opsin displayed a more diffuse staining (**E**) that overlapped with cone arrestin. However, blue opsin localization was mostly to the cone cell boundaries (**K**, *arrows*). Overlaid images are shown in **C**, **F**, **I**, **L**. Scale bar, 40 μm.

Data presented in this study demonstrated that the RPE65 donor retinas showed generalized loss of rod and cone photoreceptors except in the central macula, with RPE thinning in most regions of the peripheral retina. Together with the data reported on LCA patients, the findings we report here, though of interest, cannot necessarily be regarded as representative of the pathology in all RPE65 mutations.

Our study probed the distribution of cone arrestin, red/green opsin, and blue opsin in the RPE65 eye and compared it with the distribution in control eyes. A previous study has shown that abnormal cones, from RP donor eyes with rhodopsin mutations, displayed loss of immunolabeling with anti–cone arrestin.[24] However, in the present RPE65 donor eye, virtually all cones that labeled with anti–cone arrestin also showed labeling with the red/green or blue opsin antibodies. This difference in cone labeling may be attributed to different pathogenic mechanisms of the involved retinal degenerations.
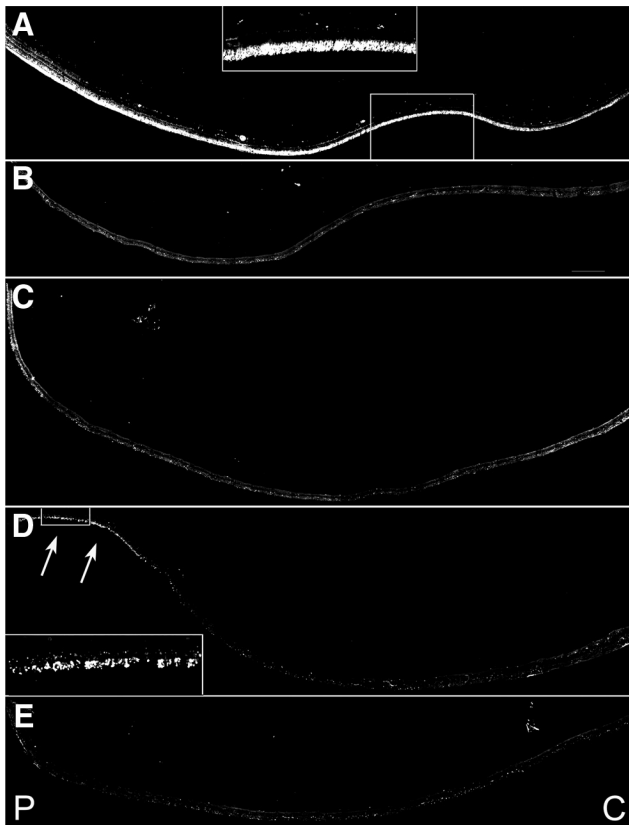
FIGURE 9. Absence of rhodopsin in the rods in the periphery of an RPE65 postmortem donor eye. Montages of photomicrographs of the periphery tissue from the RPE65 donor (**B–E**) and control eyes (**A**) were analyzed using a rhodopsin antibody (B630N). Comparison of the samples showed that rhodopsin was mostly absent in the affected retina in the inferior (**B**), superior (**C**), and nasal (**E**) regions. A few rods were still present in the far periphery of the temporal region of the RPE65 mutant retina (**D**, *inset* and *arrows*). P, periphery; C, central. Scale bar, 500 μm.

Our data show that the better visual acuity the patient had in the right eye when tested 5 years earlier suggests that very few cones are required for 20/200 vision. In addition, we observed degeneration of the optic nerve and an indistinct ganglion cell layer. This is consistent with previous reports describing optic atrophy or optic pallor as one of the features associated with some forms of LCA.[15,25–31]

Previously, Porto et al.[32] published a histopathologic description of a voluntarily aborted 33-week-old fetus with LCA caused by a homozygous Cyst330Tyr missense mutation in RPE65. The fetal retina displayed reduced photoreceptor density, a thin ONL, decreased rod and cone opsin immunoreactivity, and aberrant synaptic and inner retinal organization. Ultrastructural examination revealed the presence of lipid and vesicular inclusions not seen in normal RPE. In addition, the Cyst330Tyr eyes demonstrated thickening, detachment, and collagen fibril disorganization in the underlying Bruch's membrane. The choroid was distended and abnormally vascularized compared with controls.[32]

The clinical findings when the patient was last examined at age 51 could be correlated with retinal histologic findings studied at age 56. The patient reported lower acuity in the right than in the left eye, probably because of the presence of a central macular hole in the right eye and optic nerve changes. The constricted fields with temporal islands and reduced full-field cone ERGs are consistent with the observation of cone photoreceptors only in the macula and far periphery. In addi-

tion, the near absence of rods was observed in the periphery of each eye, which is consistent with the elevated final dark-adaptation threshold of 3.5 log units. The decrease in the size of the full-field 30-Hz cone ERGs from 8.0 to 0.5 μV over 28 years suggested an exponential rate of decline of approximately 10% loss of remaining cone function per year that has been described for persons with retinitis pigmentosa.[33] The clinical description of our patient is similar to that of other RPE65 LCA patients previously described and includes measurable visual acuities, Goldmann visual fields, and small ERG amplitudes followed by slow deterioration of their visual function when measured over 20 years.[8,15]

Our study revealed a significant decrease in the accumulation of autofluorescent material in the RPE in the macula and periphery and is in agreement with observations carried out in LCA patients and in RPE65 knockout mice. Autofluorescence measures lipofuscin accumulation in the RPE, which is related to shed photoreceptor disc segments and requires vitamin A derivatives (retinoids). It allows for the visualization of disease-specific distributions of lipofuscin in the RPE, often not visible on ophthalmoscopy. Lorenz et al.[34] found absent or minimal autofluorescence in all LCA patients with compound heterozygous or homozygous RPE65 mutations, whereas autofluores-
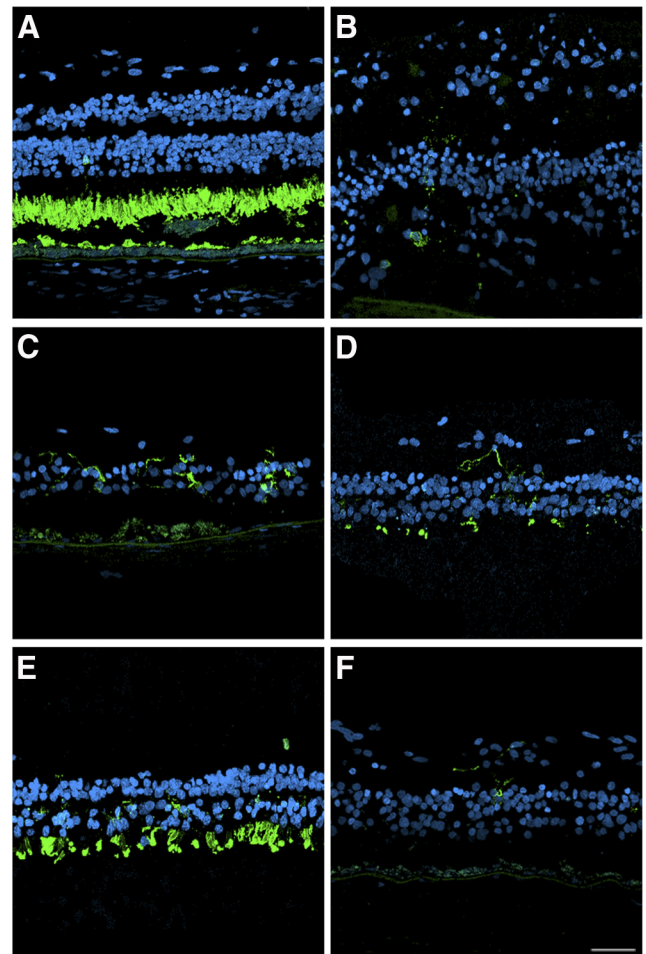
FIGURE 10. Disorganized morphology of the rods remaining in the retina of an RPE65 postmortem donor eye. High-magnification comparison of the control and RPE65 donor retina showed that rhodopsin was restricted to the rod outer segments in the control retina (**A**). In the RPE65 donor, rods were significantly decreased in the affected retina in the macula (**B**) and periphery in the inferior (**C**), superior (**D**), temporal (**E**), and nasal (**F**) quadrants, with the remaining rods expanding horizontally into the RPE65 mutant retina. Scale bar, 40 μm.
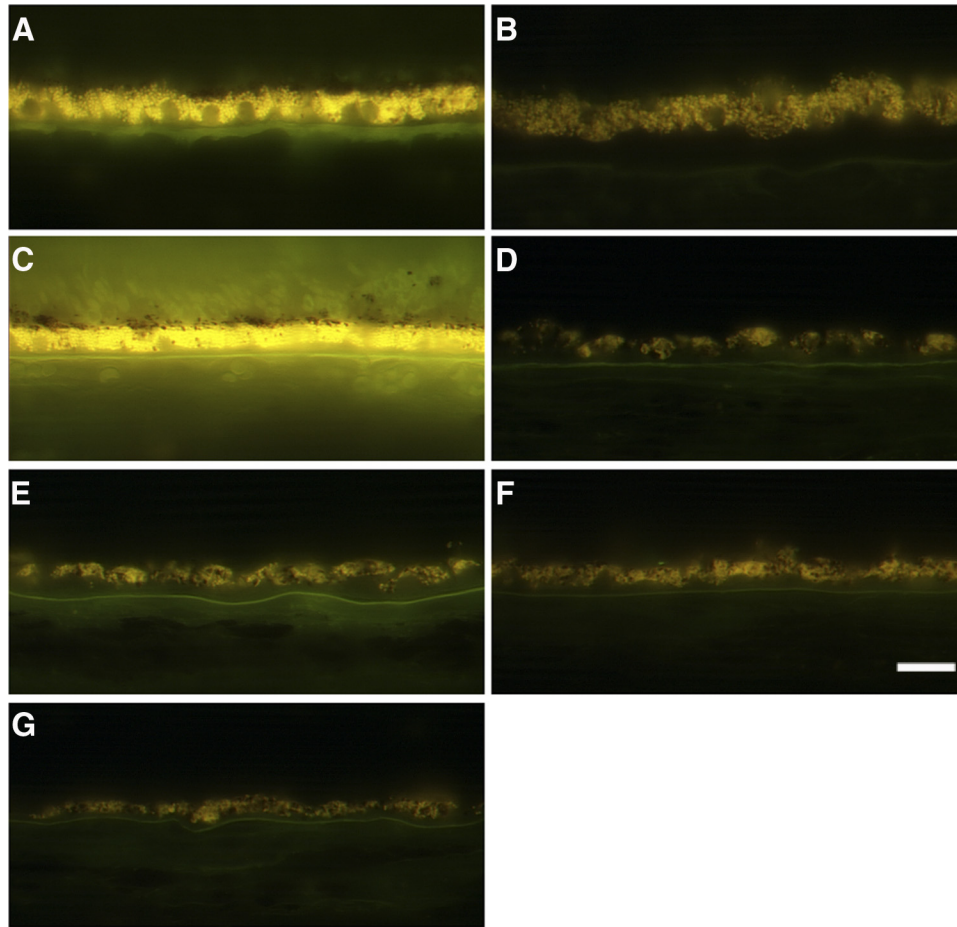
Figure 11. Significant decrease in the accumulation of autofluorescent material in the RPE of an RPE65 postmortem donor eye. Human cryosections of both a matched control (**A**, **C**) and an affected RPE65 donor (**B**, **D–G**) were observed on epifluorescence in the green channel (FITC filter, excitation 495 nm/emission 519 nm). RPE from the RPE65 mutant retina displayed significantly decreased autofluorescent granules in the macula (**B**) and periphery in the inferior (**D**), superior (**E**), temporal (**F**), and nasal (**G**) quadrants when compared with the control RPE (**A**). Scale bar, 200 μm.

cence was normal in the heterozygous parents and in LCA patients without mutations in RPE65 but with GUCY2D mutations. In the *Rpe65* knockout mice, RPE lipofuscin fluorophore accumulation was almost abolished in 12- to 13-month-old mice, indicating that the formation of RPE lipofuscin fluorophores is almost completely dependent on a normal visual cycle.[35,36]

The immunoreactivity of the RPE in the RPE65 postmortem donor eye when probed with the RPE65 antibody clearly indicates that RPE65 protein was present in this tissue. Although the functional consequences of the Ala132Thr substitution in the protein caused by the specific mutation in the *RPE65* gene of this donor are unknown, the severe progressive loss of rod and cone photoreceptors documented during her life suggests that this mutation results in the production of nonfunctional or minimally functional retinol isomerase by the RPE cells. Because some functional vision was retained in the remaining cones of the macula, a question arises about the source of the retinol isomerase that produces the chromophore used by these foveal cones. Recent studies[37,38] provide evidence that in addition to the retinol isomerase in the RPE (RPE65), there is another pathway in the outer retina for the generation of 11-*cis* retinoid used by cone photoreceptors that is independent of RPE65 activity. It is possible that some foveal cones in this RPE65 postmortem donor eye retained function because of the presence of this other pathway for the generation of a photo-

active chromophore. Alternatively, although all cones failed comparably, the fovea failed last possibly because the density of cones was highest in this region.

Recently, two-photon microscopy revealed specialized storage sites for retinyl esters that were referred to as retinosomes or retinyl ester storage particles, taking advantage of the intrinsic fluorescence of all-*trans* retinyl esters in the living mouse eye.[39–41] Retinosomes were shown to correspond to vacuole-like structures, with translucent inclusions observed with electron microscopy. Our observations of the ultrastructure in this RPE65 donor eye revealed the presence of several cytoplasmic pleomorphic inclusions similar in structure to the retinosomes described in the RPE of wild-type and RPE65$^{-/-}$ mice. However, because the detection of retinosomes is carried out in vivo, we could not confirm the presence of these structures in the RPE of the RPE65 postmortem donor eye.

Several animal models with RPE65 mutations have been characterized and used in studies that have advanced our knowledge of LCA. In the knockout mouse model of the *RPE65* gene, RPE$^{-/-}$, rods and cones are present at birth and appear normal with intact outer segments until 15 weeks; however, the outer nuclear layer displays only seven layers at 28 weeks. The rod ERG is absent from the beginning, but the cone ERG is intact. Furthermore, the rhodopsin molecule is absent.[6] Therefore, the RPE$^{-/-}$ mouse model likely represents a rod-cone degeneration, with much more rod than cone dis-
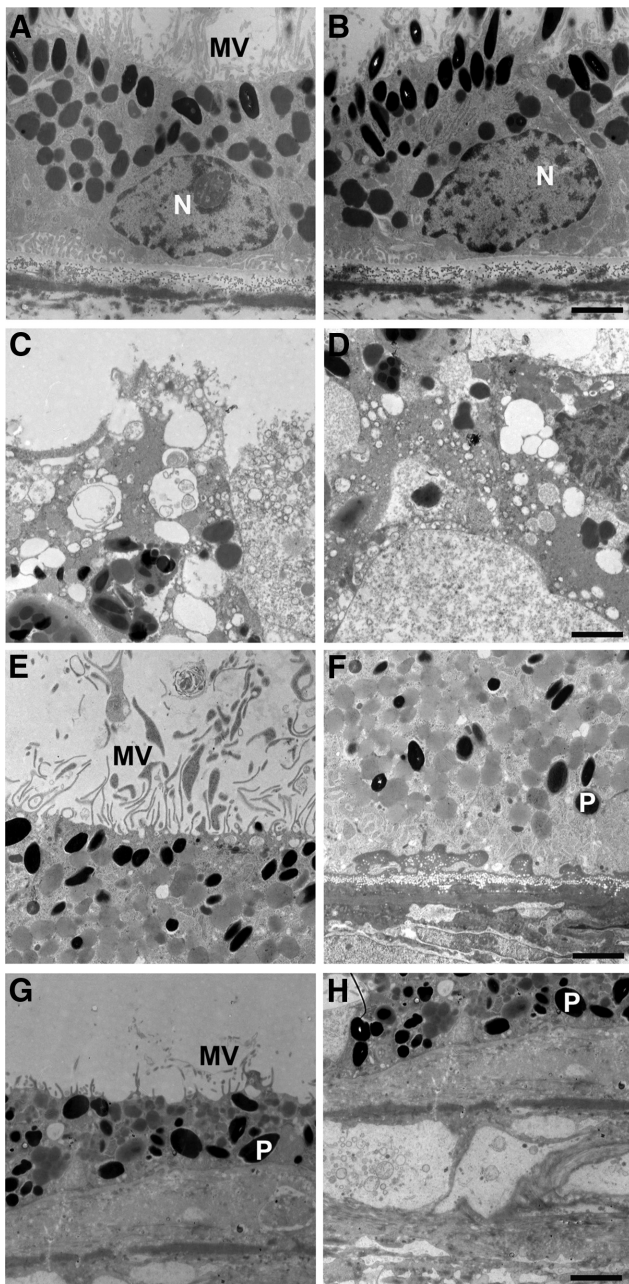
FIGURE 12. RPE degeneration in an RPE65 postmortem donor eye. Electron micrographs of the RPE from the control (**A**, **B**) and the RPE65 donor (**C–H**). The control RPE displayed apical microvilli (**A**) and basal infoldings (**B**). The ultrastructure of the RPE65 donor RPE showed degenerating changes in the different quadrants studied. In the macula, apical microvilli were absent, and pleomorphic inclusions were common (**C**). The basal surface was characterized by the absence of infoldings and pleomorphic inclusions (**D**). In the nasal quadrant, apical microvilli were present (**E**). However, the basal surface was characterized by the presence of electron-dense material beneath the RPE cells (**F**). In the inferior quadrant, the RPE was discontinuous, and in some areas short apical microvilli were still present above the RPE (**G**) and a debris zone was present below it (**H**). N, nucleus; P, pigment; MV, microvilli. Scale bars, 2 μm.

ease, and therefore is a good model for human LCA. On the other hand, the Briard dog displays a natural knockout of the *RPE65* gene that includes a 4-bp deletion of the gene.[42,43] In this model the retinal appearance of young animals is mostly normal, with the exception of the presence of inclusion bodies

in the RPE layer; however, the ERG of both cones and rods is undetectable. This model is characterized by a very slow progressive retinal degeneration with outer segment shortening and retinal thinning.

In animals with RPE65 deficiency, gene transfer resulted in efficient RPE transduction, close to normal levels of rhodopsin and 11-*cis* retinal, and improved ERG responses with consequent improved visual acuity and visual guided behavior leading the way to consideration of human trials for this potentially reversible biochemical defect.[17,44–55] At first, three clinical trials involved the administration of adenoassociated virus vectors to replace for RPE65 deficiency and included nine patients.[56–58] All the trials targeted the clinically worse eye of adult patients with advanced disease. The short-term results from these ongoing trials were recently reported with improvements in light sensitivity, ambulation through an obstacle course, and nystagmus frequency in some patients, but the results were less promising in other patients. All patients still had nonrecordable ERGs, which was in clear contrast to the results obtained in the treatment studies using the canine model of RPE65 deficiency.[56–58]

Since the first clinical trial results were reported,[56–58] clinical data on >30 patients are now available. As expected, the clinical benefit remained stable in all patients, and no severe adverse effects were observed.[59,60] Overall, younger patients responded better to treatment and had greater improvements in light sensitivity than older patients.[60,61] Because of the extensive loss of photoreceptors, the degeneration of the optic nerve, and the indistinct ganglion cell layer observed in the retina of the RPE65 donor described here, it seems unlikely that gene therapy would result in extensive recovery of vision in a patient with retinal degeneration this advanced.

References

1. Cremers FP, van den Hurk JA, den Hollander AI. Molecular genetics of Leber congenital amaurosis. *Hum Mol Genet.* 2002;11:1169–1176.
2. den Hollander AI, Roepman R, Koenekoop RK, Cremers FP. Leber congenital amaurosis: genes, proteins and disease mechanisms. *Prog Retin Eye Res.* 2008;27:391–419.
3. Jin M, Li S, Moghrabi WN, Sun H, Travis GH. Rpe65 is the retinoid isomerase in bovine retinal pigment epithelium. *Cell.* 2005;122:449–459.
4. Moiseyev G, Chen Y, Takahashi Y, Wu BX, Ma JX. RPE65 is the isomerohydrolase in the retinoid visual cycle. *Proc Natl Acad Sci U S A.* 2005;102:12413–12418.
5. Redmond TM, Poliakov E, Yu S, Tsai JY, Lu Z, Gentleman S. Mutation of key residues of RPE65 abolishes its enzymatic role as isomerohydrolase in the visual cycle. *Proc Natl Acad Sci U S A.* 2005;102:13658–13663.
6. Redmond TM, Yu S, Lee E, et al. Rpe65 is necessary for production of 11-cis-vitamin A in the retinal visual cycle. *Nat Genet.* 1998;20:344–351.
7. Woodruff ML, Olshevskaya EV, Savchenko AB, et al. Constitutive excitation by Gly90Asp rhodopsin rescues rods from degeneration caused by elevated production of cGMP in the dark. *J Neurosci.* 2007;27:8805–8815.
8. Dharmaraj SR, Silva ER, Pina AL, et al. Mutational analysis and clinical correlation in Leber congenital amaurosis. *Ophthalmic Genet.* 2000;21:135–150.
9. Marlhens F, Bareil C, Griffoin JM, et al. Mutations in RPE65 cause Leber's congenital amaurosis. *Nat Genet.* 1997;17:139–141.
10. Perrault I, Rozet JM, Ghazi I, et al. Different functional outcome of RetGC1 and RPE65 gene mutations in Leber congenital amaurosis. *Am J Hum Genet.* 1999;64:1225–1228.
11. Gu SM, Thompson DA, Srikumari CR, et al. Mutations in RPE65 cause autosomal recessive childhood-onset severe retinal dystrophy. *Nat Genet.* 1997;17:194–197.
12. Morimura H, Fishman GA, Grover SA, Fulton AB, Berson EL, Dryja TP. Mutations in the RPE65 gene in patients with autosomal re-

cessive retinitis pigmentosa or Leber congenital amaurosis. *Proc Natl Acad Sci U S A*. 1998;95:3088–3093.

13. Thompson DA, Gal A. Vitamin A metabolism in the retinal pigment epithelium: genes, mutations, and diseases. *Prog Retin Eye Res*. 2003;22:683–703.

14. Cai X, Conley SM, Naash MI. RPE65: role in the visual cycle, human retinal disease, and gene therapy. *Ophthalmic Genet*. 2009;30:57–62.

15. Lorenz B, Gyurus P, Preising M, et al. Early-onset severe rod-cone dystrophy in young children with RPE65 mutations. *Invest Ophthalmol Vis Sci*. 2000;41:2735–2742.

16. Paunescu K, Wabbels B, Preising MN, Lorenz B. Longitudinal and cross-sectional study of patients with early-onset severe retinal dystrophy associated with RPE65 mutations. *Graefes Arch Clin Exp Ophthalmol*. 2005;243:417–426.

17. Acland GM, Aguirre GD, Ray J, et al. Gene therapy restores vision in a canine model of childhood blindness. *Nat Genet*. 2001;28:92–95.

18. Dejneka NS, Surace EM, Aleman TS, et al. In utero gene therapy rescues vision in a murine model of congenital blindness. *Mol Ther*. 2004;9:182–188.

19. Jacobson SG, Aleman TS, Cideciyan AV, et al. Identifying photoreceptors in blind eyes caused by RPE65 mutations: prerequisite for human gene therapy success. *Proc Natl Acad Sci U S A*. 2005;102:6177–6182.

20. Jacobson SG, Aleman TS, Cideciyan AV, et al. Human cone photoreceptor dependence on RPE65 isomerase. *Proc Natl Acad Sci U S A*. 2007;104:15123–15128.

21. Jacobson SG, Cideciyan AV, Aleman TS, et al. RDH12 and RPE65, visual cycle genes causing Leber congenital amaurosis, differ in disease expression. *Invest Ophthalmol Vis Sci*. 2007;48:332–338.

22. Jacobson SG, Cideciyan AV, Aleman TS, et al. Photoreceptor layer topography in children with Leber congenital amaurosis caused by RPE65 mutations. *Invest Ophthalmol Vis Sci*. 2008;49:4573–4577.

23. Jacobson SG, Aleman TS, Cideciyan AV, et al. Defining the residual vision in Leber congenital amaurosis caused by RPE65 mutations. *Invest Ophthalmol Vis Sci*. 2009;50:2368–2375.

24. John SK, Smith JE, Aguirre GD, et al. Loss of cone molecular markers in rhodopsin-mutant human retinas with retinitis pigmentosa. *Mol Vis*. 2000;6:204–215.

25. Gillespie FD. Congenital amaurosis of Leber. *Am J Ophthalmol*. 1966;61:874–880.

26. Flynn JT, Cullen RF. Disc oedema in congenital amaurosis of Leber. *Br J Ophthalmol*. 1975;59:497–502.

27. Noble KG, Carr RE. Peripapillary pigmentary retinal degeneration. *Am J Ophthalmol*. 1978;86:65–75.

28. Moore A. Inherited retinal dystrophies. In: Taylor D, ed. *Pediatric Ophthalmology*. Boston: Blackwell Scientific Publications; 1990:376–406.

29. Koenekoop RK. An overview of Leber congenital amaurosis: a model to understand human retinal development. *Surv Ophthalmol*. 2004;49:379–398.

30. Booij JC, Florijn RJ, ten Brink JB, et al. Identification of mutations in the AIPL1, CRB1, GUCY2D, RPE65, and RPGRIP1 genes in patients with juvenile retinitis pigmentosa. *J Med Genet*. 2005;42:1–8.

31. Sullivan TJ, Lambert SR, Buncic JR, Musarella MA. The optic disc in Leber congenital amaurosis. *J Pediatr Ophthalmol Strabismus*. 1992;29:246–249.

32. Porto FB, Perrault I, Hicks D, et al. Prenatal human ocular degeneration occurs in Leber's congenital amaurosis (LCA2). *J Gene Med*. 2002;4:390–396.

33. Berson EL. Long-term visual prognoses in patients with retinitis pigmentosa: the Ludwig von Sallmann lecture. *Exp Eye Res*. 2007;85:7–14.

34. Lorenz B, Wabbels B, Wegscheider E, Hamel CP, Drexler W, Preising MN. Lack of fundus autofluorescence to 488 nanometers from childhood on in patients with early-onset severe retinal dystrophy associated with mutations in RPE65. *Ophthalmology*. 2004;111:1585–1594.

35. Katz ML, Redmond TM. Effect of Rpe65 knockout on accumulation of lipofuscin fluorophores in the retinal pigment epithelium. *Invest Ophthalmol Vis Sci*. 2001;42:3023–3030.

36. Katz ML, Wendt KD, Sanders DN. RPE65 gene mutation prevents development of autofluorescence in retinal pigment epithelial phagosomes. *Mech Ageing Dev*. 2005;126:513–521.

37. Mata NL, Radu RA, Clemmons RC, Travis GH. Isomerization and oxidation of vitamin a in cone-dominant retinas: a novel pathway for visual-pigment regeneration in daylight. *Neuron*. 2002;36:69–80.

38. Mata NL, Ruiz A, Radu RA, Bui TV, Travis GH. Chicken retinas contain a retinoid isomerase activity that catalyzes the direct conversion of all-trans retinol to 11-cis retinol. *Biochemistry*. 2005;44:11715–11721.

39. Imanishi Y, Batten ML, Piston DW, Baehr W, Palczewski K. Noninvasive two-photon imaging reveals retinyl ester storage structures in the eye. *J Cell Biol*. 2004;164:373–383.

40. Imanishi Y, Gerke V, Palczewski K. Retinosomes: new insights into intracellular managing of hydrophobic substances in lipid bodies. *J Cell Biol*. 2004;166:447–453.

41. Imanishi Y, Lodowski KH, Koutalos Y. Two-photon microscopy: shedding light on the chemistry of vision. *Biochemistry*. 2007;46:9674–9684.

42. Wrigstad A, Narfstrom K, Nilsson SE. Slowly progressive changes of the retina and retinal pigment epithelium in Briard dogs with hereditary retinal dystrophy: a morphological study. *Doc Ophthalmol*. 1994;87:337–354.

43. Aguirre GD, Baldwin V, Pearce-Kelling S, Narfstrom K, Ray K, Acland GM. Congenital stationary night blindness in the dog: common mutation in the RPE65 gene indicates founder effect. *Mol Vis*. 1998;4:23.

44. Narfstrom K, Katz ML, Ford M, Redmond TM, Rakoczy E, Bragadottir R. In vivo gene therapy in young and adult RPE65−/− dogs produces long-term visual improvement. *J Hered*. 2003;94:31–37.

45. Lai CM, Yu MJ, Brankov M, et al. Recombinant adeno-associated virus type 2-mediated gene delivery into the Rpe65−/− knockout mouse eye results in limited rescue. *Genet Vaccines Ther*. 2004;2:3.

46. Acland GM, Aguirre GD, Bennett J, et al. Long-term restoration of rod and cone vision by single dose rAAV-mediated gene transfer to the retina in a canine model of childhood blindness. *Mol Ther*. 2005;12:1072–1082.

47. Narfstrom K, Vaegan, Katz M, Bragadottir R, Rakoczy EP, Seeliger M. Assessment of structure and function over a 3-year period after gene transfer in RPE65−/− dogs. *Doc Ophthalmol*. 2005;111:39–48.

48. Bemelmans AP, Kostic C, Crippa SV, et al. Lentiviral gene transfer of RPE65 rescues survival and function of cones in a mouse model of Leber congenital amaurosis. *PLoS Med*. 2006;3:e347.

49. Nusinowitz S, Ridder WH 3rd, Pang JJ, et al. Cortical visual function in the rd12 mouse model of Leber congenital amaurosis (LCA) after gene replacement therapy to restore retinal function. *Vision Res*. 2006;46:3926–3934.

50. Pang JJ, Chang B, Kumar A, et al. Gene therapy restores vision-dependent behavior as well as retinal structure and function in a mouse model of RPE65 Leber congenital amaurosis. *Mol Ther*. 2006;13:565–572.

51. Rolling F, Le Meur G, Stieger K, et al. Gene therapeutic prospects in early onset of severe retinal dystrophy: restoration of vision in RPE65 Briard dogs using an AAV serotype 4 vector that specifically targets the retinal pigmented epithelium. *Bull Mem Acad R Med Belg*. 2006;161:497–508, discussion 508–499.

52. Aguirre GK, Komaromy AM, Cideciyan AV, et al. Canine and human visual cortex intact and responsive despite early retinal blindness from RPE65 mutation. *PLoS Med*. 2007;4:e230.

53. Le Meur G, Stieger K, Smith AJ, et al. Restoration of vision in RPE65-deficient Briard dogs using an AAV serotype 4 vector that specifically targets the retinal pigmented epithelium. *Gene Ther*. 2007;14:292–303.

54. Roman AJ, Boye SL, Aleman TS, et al. Electroretinographic analyses of Rpe65-mutant rd12 mice: developing an in vivo bioassay for human gene therapy trials of Leber congenital amaurosis. *Mol Vis*. 2007;13:1701–1710.

55. Bennicelli J, Wright JF, Komaromy A, et al. Reversal of blindness in animal models of Leber congenital amaurosis using optimized AAV2-mediated gene transfer. *Mol Ther*. 2008;16:458–465.

56. Bainbridge JW, Ali RR. Success in sight: the eyes have it! Ocular gene therapy trials for LCA look promising. *Gene Ther.* 2008;15: 1191–1192.

57. Hauswirth WW, Aleman TS, Kaushal S, et al. Treatment of Leber congenital amaurosis due to RPE65 mutations by ocular subretinal injection of adeno-associated virus gene vector: short-term results of a phase I trial. *Hum Gene Ther.* 2008;19:979–990.

58. Maguire AM, Simonelli F, Pierce EA, et al. Safety and efficacy of gene transfer for Leber's congenital amaurosis. *N Engl J Med.* 2008;358:2240–2248.

59. Cideciyan AV, Hauswirth WW, Aleman TS, et al. Human RPE65 gene therapy for Leber congenital amaurosis: persistence of early visual improvements and safety at 1 year. *Hum Gene Ther.* 2009; 20:999–1004.

60. Simonelli F, Maguire AM, Testa F, et al. Gene therapy for Leber's congenital amaurosis is safe and effective through 1.5 years after vector administration. *Mol Ther.* 2010;18:643–650.

61. Maguire AM, High KA, Auricchio A, et al. Age-dependent effects of RPE65 gene therapy for Leber's congenital amaurosis: a phase 1 dose-escalation trial. *Lancet.* 2009;374:1597–1605.